Eur. Phys. J. D **33**, 413–420 (2005)
DOI: 10.1140/epjd/e2005-00076-x

THE EUROPEAN PHYSICAL JOURNAL D

A cluster study of aluminum adsorption on Ga-rich GaAs(100)(2 × 1) and β(4 × 2) surfaces

M.L. Mayo and A.K. Ray[a]

Physics Department, University of Texas at Arlington, Arlington, Texas 76019, USA

Received 14 September 2004 / Received in final form 24 January 2005
Published online 24 May 2005 –

Abstract. Ab initio self-consistent total energy calculations using second order Møller-Plesset perturbation theory and Hay-Wadt effective core potentials with associated basis sets (HWECP's) for gallium and arsenic have been used to investigate the chemisorption properties of atomic aluminum on the Ga-rich GaAs(100)-(2 × 1) and β(4 × 2) surfaces. Finite sized hydrogen saturated clusters with the experimental zinc-blende lattice constant of 5.654 Å and the energy optimized Ga dimer bond length of 2.758 Å have been used to model the semiconductor surface. To investigate the effects of the core electrons of aluminum in the adsorption process, we have represented the Al adatom with both HWECP's and an all electron 6-311++G** basis set. Detailed energetics of chemisorption on the (100) surface, including chemisorption energies, nearest surface neighbor bond lengths, and Mulliken population analysis, have been reported for all considered sites of chemisorption.

PACS. 36.40.-c Atomic and molecular clusters – 71.15.-m Methods of electronic structure calculations – 71.15.Nc Total energy and cohesive energy calculations

1 Introduction

The technological applications of GaAs due to its high electron mobility and direct band gap make it an important system for fundamental and applied research. The industry standard for growing GaAs by molecular beam epitaxy (MBE) is the (100) surface. This surface has the highest aerial density of dangling surface bonds, greater than the corresponding density of the (110) or (111) surface and consequently, surface reconstruction is facilitated by these bonds. In this work, we extend our previous work on atomic hydrogen, oxygen, and cesium adsorptions on the Ga-rich GaAs(100) surface [1,2] to study aluminum adsorption on the GaAs(100) surface. As is known, metal-semiconductor interfaces have been of major interest to both experimentalists and theoreticians for an understanding of Ohmic and Schottky barrier contacts and also for extensive industrial applications of semiconductor devices [3–9]. Al-GaAs, in particular, is used extensively in the electronics industry in integrated circuitry and optoelectronic devices. This Al-GaAs interface has been the subject of ongoing research for several decades and at room temperature over time, it is believed that Al undergoes an exchange reaction with surface Ga atoms on the GaAs surface. Ludeke et al. [8] used Auger spectroscopy to study the interface behavior and crystallographic relationships of aluminum on the GaAs(100)-$c(2 \times 8)$ and the Ga-rich (4×6) surfaces. They observed notable differences in the degrees of interface reactivity and crystallographic relationships to Al over-layers on the reconstructed surfaces. No replacement reaction was detected for the $c(2 \times 8)$ surface at room temperature and only a partial exchange reaction was observed for the (4×6) surface. Chen et al. [9] studied ultra thin films of aluminum deposited on GaAs(100) using positron annihilation induced auger electron spectroscopy and electron induced auger electron spectroscopy. They found direct evidence that Ga substitutes for Al in the top layer after Al deposition and that Ga diffuses into the Al over-layer faster than As. The sensitivity of PAES allowed them to directly monitor the time evolution of the changes in the top layer of an Al layer deposited on GaAs.

Apart from the Al-GaAs interaction, the Ga-rich GaAs(100) surface and possible reconstructions and relaxations thereof have also been the focus of ongoing research and controversy for several decades [10–19]. Bacharach et al. [10] have shown experimentally that a (2×1) periodicity on the GaAs(100) surface is observed when a fraction of a monolayer of Al is deposited on the surface. As noted by Lee et al. [17], the GaAs(001)-$c(8 \times 2)$ surface is built from (4×2) structural units. In this study, we consider several (2×1) reconstructions and the $\beta(4 \times 2)$ reconstruction of which the (2×1) reconstructions can be considered structural sub-units. Kumpf et al. [18] studied the

[a] e-mail: akr@uta.edu

structure of metal-rich (001) surfaces of III-V compound semiconductors with X-ray diffraction using direct methods. They found that the atomic structure of the $c(8 \times 2)$ reconstruction, as related to the GaAs-(001) surface, is characterized by subsurface dimerization of Ga-atoms in the second bi-layer and Ga-dimers in the top layer. Recently, Seino et al. [19] investigated the structure and energetics of Ga-rich GaAs(001) surfaces. Their first-principles total-energy calculations, based on a real-space finite difference implementation of the density functional theory in the local-density approximation using norm-conserving pseudo-potentials, suggest the occurrence of the Ga-rich (4×2) surface. However, they found that the (4×6) reconstructions proposed to explain STM experiments were unstable.

The above brief summary indicates that various possible reconstructions and relaxations of the Ga-rich GaAs(100) surface have been proposed in the literature and to some extent, the models of reconstruction and relaxation depends on the experimental and theoretical techniques used. Here, we investigate the possible Al adsorption sites and the nature of the GaAs surface upon adsorption on the (2×1) and $\beta(4 \times 2)$ surface reconstructions which, as previously mentioned, can be considered as structural subunits of the $c(8 \times 2)$ surface as an *initial* attempt towards a better understanding of Al-GaAs interactions. As such, we have not considered surface and subsurface relaxations in the present study. The semiconductor surfaces in this study, as in our previous works [1,2], are represented by a three-layer cluster model. A similar three layer cluster approach has recently been used by Kunsági-Máté et al. [20] to study the As-Ga surface exchange on the As-rich GaAs(001) reconstructed surface. We note that clusters are well suited for the study of metal and semiconductor surfaces and adsorptions on them and in general can yield accurate results of such properties as the chemical nature of the bond, bond length, chemisorption energies and other electronic and geometric structure properties [21–24]. Our study as reported here is, to the best of our knowledge, the *first ab initio cluster study of atomic Al adsorption on the Ga-rich GaAs(100) surface using cluster models.* Specifically investigated are the adsorption sites, chemisorption energies, possibilities of charge transfers between the adatom and the Ga and the As atoms and also the highest occupied molecular orbital-lowest unoccupied molecular orbital (HOMO-LUMO) gaps. We first comment on the computational methodology followed by results.

2 Computational methodology and results

Both the unrestricted Hartree–Fock (UHF) theory and the many-body perturbation theory (MBPT) as used in this work are well documented in the literature [25–29]. In this work, because of severe demands on computational resources, we have carried out complete unrestricted second-order many-body perturbation theory (UMP2) calculations, which consist of all single and double-excitation terms for both the bare clusters and the chemisorbed systems. One of the primary considerations involved in ab initio calculations is the type of basis set to be used [30]. Basis sets used in ab initio molecular-orbital computations usually involve some compromise between computational cost and accuracy. Keeping in mind the tremendous cost of ab initio calculations, specifically for large systems like gallium, and arsenic, we have elected to represent them by effective core potentials or pseudopotentials. In particular, we have used the Hay-Wadt effective core potentials (HWECP) and associated basis sets for aluminum, gallium, and arsenic atoms [31]. These core potentials are known to provide excellent agreement with all electron results. To further improve the accuracy of our calculations, one d function was added to the Hay-Wadt basis sets. The exponents of the d functions were chosen to provide minimum energy for the Ga_2, As_2, and Al_2 dimers with the bond lengths fixed at experimental values [32]. The values for the exponents for gallium and arsenic were found to be $d_{Ga} = 0.170$ and $d_{As} = 0.280$ respectively. This procedure has been previously used in our studies of alkali adsorptions on the GaAs(110) surface. The value of the exponent for aluminum is found to be $d_{Al} = 0.218$. For hydrogen, a $[2s, 1p]$ basis set was used. With these basis sets, we have also estimated the basis set superposition error (BSSE), using the methods Dimon et al. and Boys and Bernardi [33]. The BSSE for a Ga_2As_2 system is found to be 0.0025 a.u. and that for a GaAlAs system is 0.0028 a.u. As such, the upper bound to the BSSE for the GaAs and AlGaAs systems is estimated to be 0.003 a.u. The effect on the total energies is, at most, in the second decimal place. However, since the adsorption/chemisorption energies are calculated as differences in total energies, we believe that the effects on these energies due to BSSE is basically negligible. All computations were carried out using the parallel version of Gaussian 98 [34] on Compaq Alpha ES20 and ES40 parallel supercomputers at the University of Texas at Arlington.

In this work, as mentioned before, we considered clusters representing two different reconstructed surfaces, namely the (2×1) and $\beta(4 \times 2)$ surfaces [1,2]. Five different clusters were constructed (Fig. 1), the smallest being the $Ga_4As_4H_{12}$ with two Ga atoms in the first layer and the largest being $Ga_{19}As_{15}H_{39}$ with nine Ga atoms in the first layer. Each cluster was constructed with Ga and As atoms located at the bulk lattice sites given by the zinc-blende structure with an experimental lattice constant of 5.654 Å. Ga atoms terminated the first or the top layer and the second layer was composed of As atoms while the third layer was composed of Ga atoms. The cluster sizes increased in transverse dimensions as well as number of layers, with the maximum number of layers being three. Hydrogen atoms have been used to saturate the dangling bonds, except above the surface, at an energy optimized bond length of 1.511 Å. This is in agreement with the work of Nonoyama et al. [35] who used a similar approach for constructing $Ga_4As_4H_{12}$ for chemisorption of atomic and molecular hydrogen on the GaAs(100) surface. The dangling bonds above the clean reconstructed

Table 1. Total energy (in a.u.) and binding energy (in eV) of the (2 × 1) and $\beta(4 \times 2)$ bare clusters.

Cluster	E_{tot}(UHF)	E_{tot}(UMP2)	E_b(UHF)	E_b(UMP2)
$Ga_4As_4H_{12}$	–38.65	–39.36	1.44	1.94
$Ga_5As_6H_{16}$	–54.72	–55.75	1.29	1.85
$Ga_7As_6H_{16}$	–58.82	–59.95	1.39	1.95
$Ga_7As_6H_{19}$	–60.58	–61.71	1.48	2.00
$Ga_{19}As_{15}H_{39}$	–149.26	–152.24	1.30	1.90

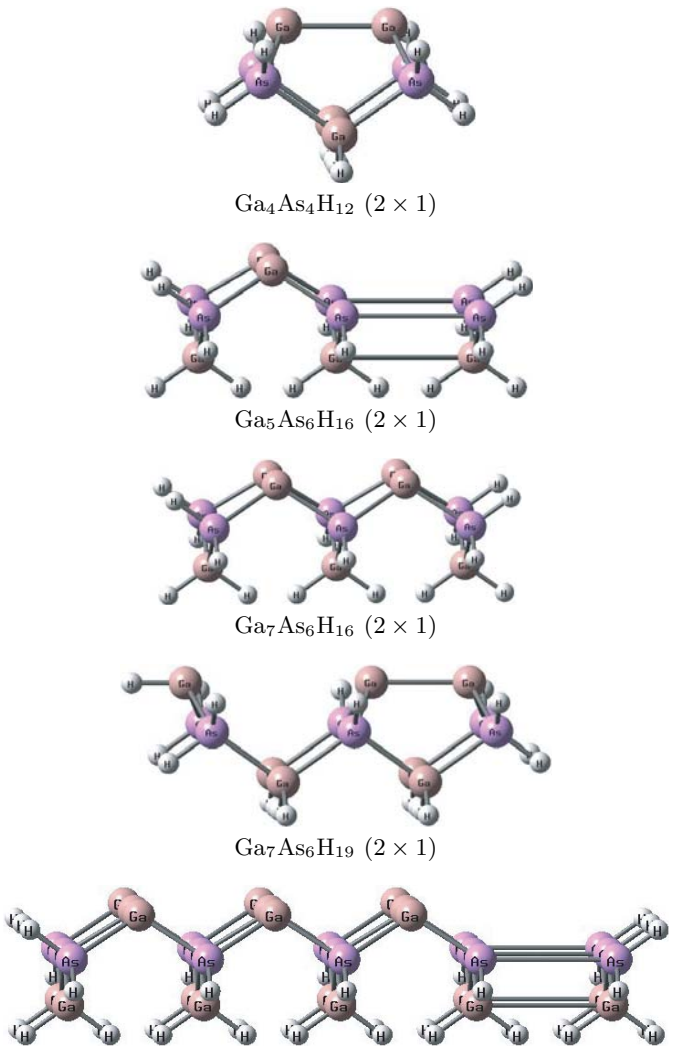

$Ga_4As_4H_{12}$ (2 × 1)

$Ga_5As_6H_{16}$ (2 × 1)

$Ga_7As_6H_{16}$ (2 × 1)

$Ga_7As_6H_{19}$ (2 × 1)

$Ga_{19}As_{15}H_{39}$ $\beta(4 \times 2)$

Fig. 1. GaAs(100) Clusters.

Ga-rich surface are then potential sites for chemisorption. Therefore, simple electron counting rules cannot be applied to these clusters since their surface bonds are not saturated. Due to severe demands on computational resources, total energy optimization was carried out only for the smallest cluster, $Ga_4As_4H_{12}$, by allowing dimerization of the surface Ga atoms. From this process, the reconstructed surface Ga-Ga dimer bond length was found to be 2.758 Å. This dimer bond length was then applied to the $Ga_5As_6H_{16}$, $Ga_7As_6H_{16}$, $Ga_7As_6H_{19}$, and $Ga_{19}As_{15}H_{39}$clusters. Specifically, the $Ga_4As_4H_{12}$, $Ga_5As_6H_{16}$, $Ga_7As_6H_{16}$, and the $Ga_7As_6H_{19}$ clusters represent the (2 × 1) surface and the $Ga_{19}As_{15}H_{39}$ cluster represents the $\beta(4 \times 2)$ surface [1,2]. Different sizes of clusters are used to represent the same surface because of non-uniqueness of a specific cluster to represent a surface and to study dependence and convergence of cluster properties with respect to cluster sizes [1]. However, for the $\beta(4 \times 2)$ surface, only one cluster is used because of the large size of the cluster. As a comparison, Guo-Ping and Ruda [36] used a surface Ga-Ga dimer bond length of 2.80 Å in a similar ab initio cluster study of the adsorption of sulfur on the Ga-rich GaAs(100) surface. They used a $Ga_7As_7H_{20}$ cluster to represent the (4 × 2), (4 × 6), and (2 × 6) surfaces and found that S atoms chemisorbed preferentially on bridge sites.

The total energies and binding energies of all the clusters at the UHF and the UMP2 levels are shown in Table 1. The binding energy per atom for a $Ga_xAs_yH_z$ cluster was calculated in the separated atom limit using the following formula,

$$E_b = (xE(\mathrm{Ga}) + yE(\mathrm{As}) + zE(\mathrm{H}) - E(\mathrm{Ga}_x\mathrm{As}_y\mathrm{H}_z))/(x + y + z). \quad (1)$$

We note that the binding energies oscillate with the number of atoms in the clusters at both levels of theory and the binding energies at the UMP2 level of theory are consistently higher than the corresponding energies at the UHF level of theory. As expected, correlation effects typically increase the binding or cohesive energy in a cluster.

In this study, we have also studied basis set effects on the chemisorption process. In addition to the pseudopotential basis set for Al, we have also used an all-electron basis set, namely a 6-311++G** basis set for Al [28,37]. We have considered five surface adsorption sites of high symmetry (Fig. 2). All sites were chosen because of their associated point symmetries. The top and bridge sites were chosen for their σ_V inversion symmetry through a plane perpendicular to the surface dimer midpoint. The cave, hollow, and trough sites were chosen for their C_{4V} point rotational symmetry about an axis normal to the (100)-plane. On the top sites 1a and 1b, the adatom is allowed to approach a path directly on top of a dimerized Ga atom. On the trough sites, the adatom is four-fold coordinated with second layer As atoms above the surface Ga vacancy. Specifically, the $Ga_5As_6H_{16}(2 \times 1)$ surface has one point of four-fold symmetry and the $Ga_{19}As_{15}H_{39}$ $\beta(4 \times 2)$ surface has two points, sites 5a and 5b, with the 5a site shown in Figure 2. To examine the relative stability of chemisorption at the different sites, the chemisorption

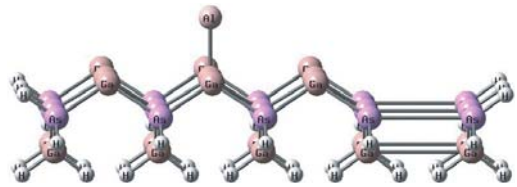

$Ga_{19}As_{15}H_{39}$ + Al Top Site 1b.

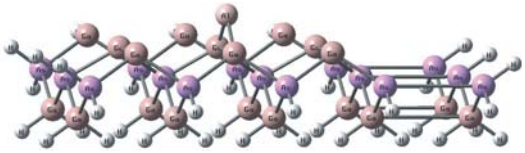

$Ga_{19}As_{15}H_{39}$ + Al Bridge Site 2.

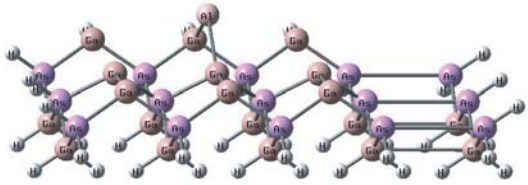

$Ga_{19}As_{15}H_{39}$ + Al Hollow Site 3.

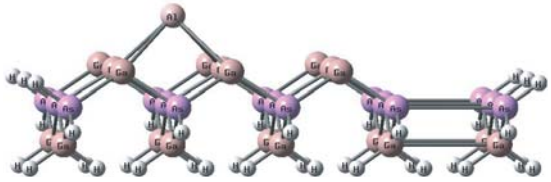

$Ga_{19}As_{15}H_{39}$ + Al Cave Site 4.

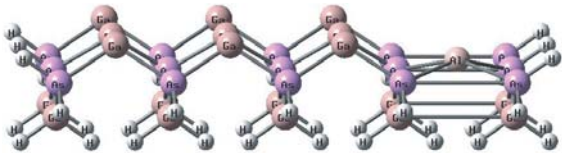

$Ga_{19}As_{15}H_{39}$ + Al Trough Site 5a.

Fig. 2. GaAs(100) chemisorbed clusters.

energies are calculated from:

$$E_c = E(\mathrm{Al}) + E(\mathrm{Ga}_x\mathrm{As}_y\mathrm{H}_z) - E(\mathrm{Al} + \mathrm{Ga}_x\mathrm{As}_y\mathrm{H}_z). \quad (2)$$

Thus, positive chemisorption energy indicates possibilities for chemisorption. For all surface sites, the height of the adatom above the top Ga layer was varied to yield the maximum chemisorption energy (i.e. a minimum of the E_c versus d curve, with the sign of the E_c changed). Typically, several data points, typically around ten, were generated with single point runs to obtain accurate values of the Al adatom distance and the chemisorption energy. Figures 3–8 show the E_c versus d curves with only a few data points around the energy minima for the sites with the highest chemisorption energy in each category.

The results at the at the unrestricted MP2 level of theory for both the HWECP's and associated basis sets augmented by a d function and the 6-311++G** basis set for aluminum are shown in Table 2. We note that all sites are potential sites for aluminum chemisorption.

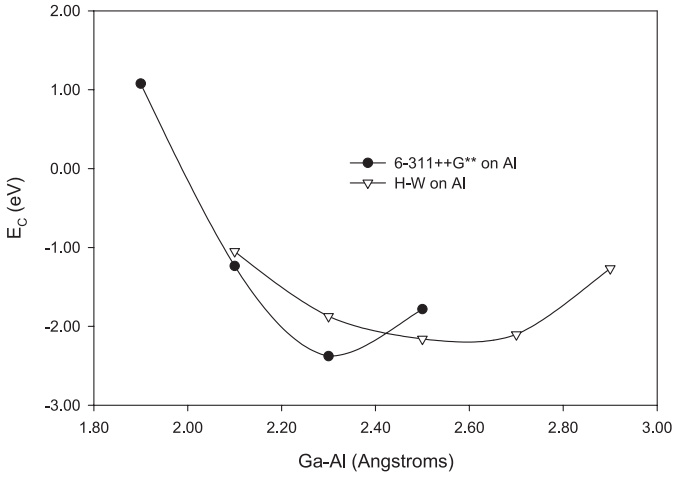

Fig. 3. Chemisorption energy vs. nearest surface neighbor bond length for $Ga_{19}As_{15}H_{39}$ + Al top site 1b.

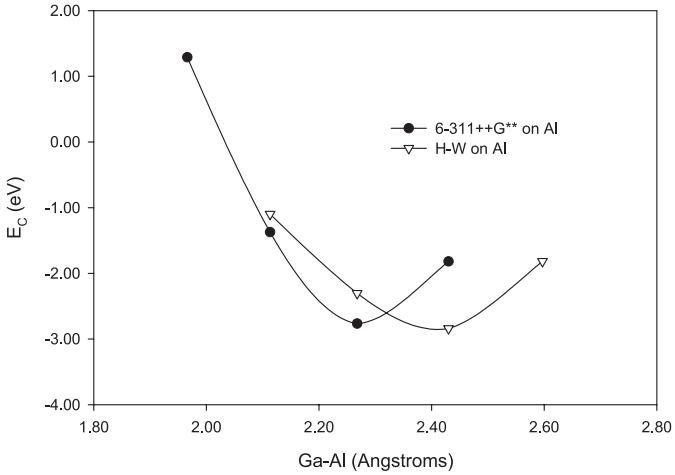

Fig. 4. Chemisorption energy vs. nearest surface neighbor bond length for $Ga_{19}As_{15}H_{39}$ + Al bridge site 2.

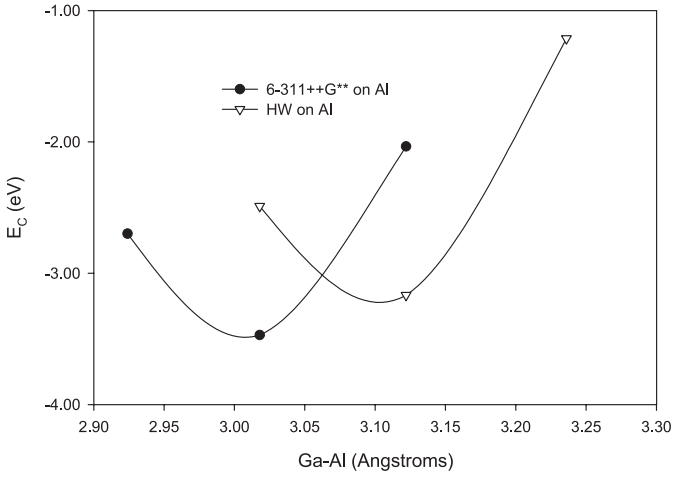

Fig. 5. Chemisorption energy vs. nearest surface neighbor bond length for $Ga_{19}As_{15}H_{39}$ + Al hollow site 3.

Table 2. Chemisorption energy (in eV) vs. cluster size and symmetry.

Site	Symmetry	Cluster	6-311++G** E_c(UMP2)	H-W E_c(UMP2)
1 (top)				
1a	2 × 1	Al + $Ga_4As_4H_{12}$	1.20	1.63
1b	2 × 1	Al + $Ga_4As_4H_{12}$	1.20	1.63
1a	2 × 1	Al + $Ga_7As_6H_{19}$	1.41	1.18
1b	2 × 1	Al + $Ga_7As_6H_{19}$	1.85	1.33
1b	4 × 2	Al + $Ga_{19}As_{15}H_{39}$	2.38	2.16
2 (bridge)	2 × 1	Al + $Ga_4As_4H_{12}$	2.33	2.25
	2 × 1	Al + $Ga_7As_6H_{19}$	2.61	2.80
	4 × 2	Al + $Ga_{19}As_{15}H_{39}$	2.77	2.84
3 (hollow)	2 × 1	Al + $Ga_7As_6H_{19}$	2.62	2.58
	4 × 2	Al + $Ga_{19}As_{15}H_{39}$	3.47	3.17
4 (cave)	2 × 1	Al + $Ga_7As_6H_{16}$	2.57	2.45
	4 × 2	Al + $Ga_{19}As_{15}H_{39}$	2.46	2.69
5 (trough)	2 × 1	Al + $Ga_5As_6H_{16}$	4.10	3.97
5a	4 × 2	Al + $Ga_{19}As_{15}H_{39}$	4.84	4.73
5b	4 × 2	Al + $Ga_{19}As_{15}H_{39}$	4.66	4.56

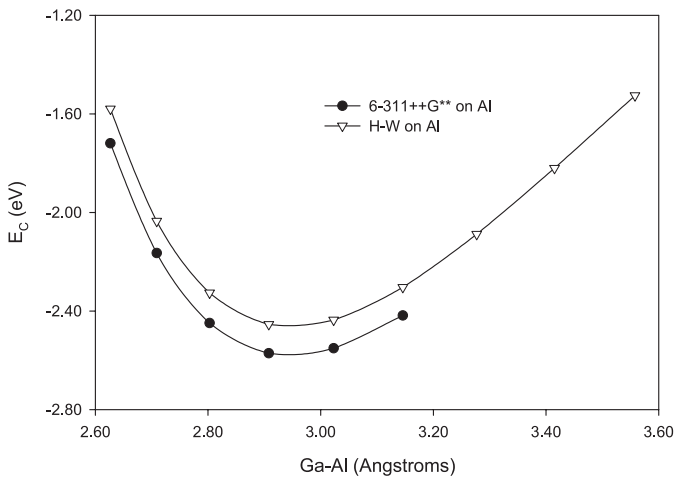

Fig. 6. Chemisorption energy vs. nearest surface neighbor bond length for $Ga_7As_6H_{16}$ + Al cave site 4.

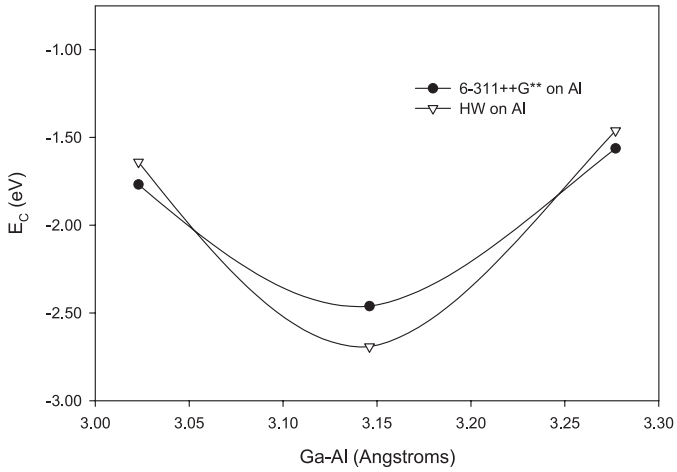

Fig. 7. Chemisorption energy vs. nearest surface neighbor bond length for $Ga_{19}As_{15}H_{39}$ + Al cave site 4.

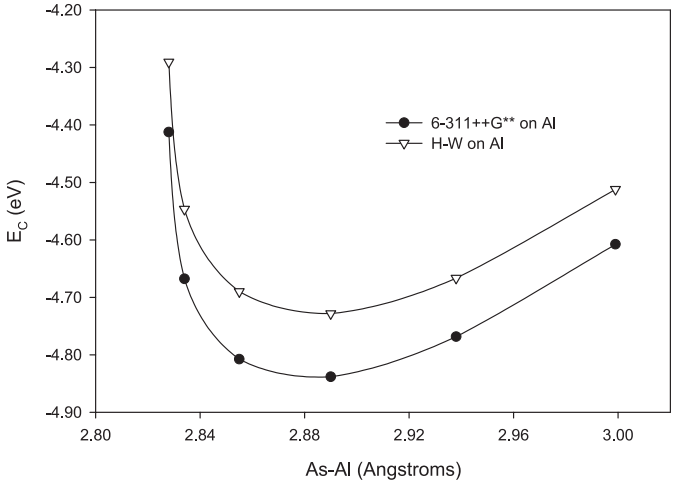

Fig. 8. Chemisorption energy vs. nearest surface neighbor bond length for $Ga_{19}As_{15}H_{39}$ + Al trough site 5a.

The chemisorption energies for the potential adsorption sites range from 1.20 eV to 4.84 eV with the 6-311++G** basis set on Al and 1.18 eV to 4.73 eV with the HWECP on Al. Also comparing the chemisorption energies of the two basis representations on the Al adatom, we find no pattern that would suggest that either basis set selection for Al yields consistently higher or lower chemisorption energies. In general, however, different basis selections yield the same predictions as to the ability for the Al adatom to chemisorb at a particular site. The highest chemisorption energies are found at the trough sites for the $Ga_5As_6H_{16}$ + Al and $Ga_{19}As_{15}H_{39}$ + Al clusters representing the (2×1) and $\beta(4\times2)$ surfaces, respectively. Notable exceptions are the lowest energy chemisorbed sites. The 6-311++G** basis on Al predicts that the $Ga_4As_4H_{12}$ + Al top sites have the lowest chemisorption energy while the HWECP representation for Al predicts that the $Ga_7As_6H_{19}$ + Al top sites yield the lower chemisorption energies. We note that the top site is rarely the preferred

Table 3. Bond length (in Å) of the Al adatom vs. cluster size and symmetry.

Sites	Symmetry	Cluster	Adatom-nearest surface neighbor bond length	Adatom-nearest surface neighbor bond length
			6-311++G**	H-W
1 (top)				
1a	2 × 1	Al + $Ga_4As_4H_{12}$	2.50	2.70
1b	2 × 1	Al + $Ga_4As_4H_{12}$	2.50	2.70
1a	2 × 1	Al + $Ga_7As_6H_{19}$	2.90	2.70
1b	2 × 1	Al + $Ga_7As_6H_{19}$	2.50	2.70
1b	4 × 2	Al + $Ga_{19}As_{15}H_{39}$	2.30	2.50
2 (bridge)	2 × 1	Al + $Ga_4As_4H_{12}$	2.68	2.68
	2 × 1	Al + $Ga_7As_6H_{19}$	2.87	2.51
	4 × 2	Al + $Ga_{19}As_{15}H_{39}$	2.27	2.43
3(hollow)	2 × 1	Al + $Ga_7As_6H_{19}$	2.80	2.80
	4 × 2	Al + $Ga_{19}As_{15}H_{39}$	3.02	3.12
4 (cave)	2 × 1	Al + $Ga_7As_6H_{16}$	2.91	2.91
	4 × 2	Al + $Ga_{19}As_{15}H_{39}$	3.15	3.15
5 (trough)	2 × 1	Al + $Ga_5As_6H_{16}$	3.12	3.12
5a	4 × 2	Al + $Ga_{19}As_{15}H_{39}$	2.89	2.89
5b	4 × 2	Al + $Ga_{19}As_{15}H_{39}$	2.89	2.89

Table 4. HOMO-LUMO gap (in eV) vs. cluster size and symmetry with 6-311++G** basis on Al.

Sites	Symmetry	Cluster	Gap	Cluster	Gap	ΔGap
1 (top)						
1a	2 × 1	$Ga_4As_4H_{12}$	7.46	Al + $Ga_4As_4H_{12}$	5.64	–1.82
1b	2 × 1	$Ga_4As_4H_{12}$	7.46	Al + $Ga_4As_4H_{12}$	5.64	–1.82
1a	2 × 1	$Ga_7As_6H_{19}$	2.06	Al + $Ga_7As_6H_{19}$	5.74	3.68
1b	2 × 1	$Ga_7As_6H_{19}$	2.06	Al + $Ga_7As_6H_{19}$	5.47	3.41
1b	4 × 2	$Ga_{19}As_{15}H_{39}$	2.39	Al + $Ga_{19}As_{15}H_{39}$	3.77	1.38
2 (bridge)	2 × 1	$Ga_4As_4H_{12}$	7.46	Al + $Ga_4As_4H_{12}$	5.50	–1.96
	2 × 1	$Ga_7As_6H_{19}$	2.06	Al + $Ga_7As_6H_{19}$	6.06	4.00
	4 × 2	$Ga_{19}As_{15}H_{39}$	2.39	Al + $Ga_{19}As_{15}H_{39}$	2.66	0.27
3 (hollow)	2 × 1	$Ga_7As_6H_{19}$	2.06	Al + $Ga_7As_6H_{19}$	6.03	3.97
	4 × 2	$Ga_{19}As_{15}H_{39}$	2.39	Al + $Ga_{19}As_{15}H_{39}$	3.60	1.21
4 (cave)	2 × 1	$Ga_7As_6H_{16}$	3.70	Al + $Ga_7As_6H_{16}$	4.40	0.70
	4 × 2	$Ga_{19}As_{15}H_{39}$	2.39	Al + $Ga_{19}As_{15}H_{39}$	2.53	0.14
5 (trough)	2 × 1	$Ga_5As_6H_{16}$	4.58	Al + $Ga_5As_6H_{16}$	5.27	0.69
5a	4 × 2	$Ga_{19}As_{15}H_{39}$	2.39	Al + $Ga_{19}As_{15}H_{39}$	2.69	0.30
5b	4 × 2	$Ga_{19}As_{15}H_{39}$	2.39	Al + $Ga_{19}As_{15}H_{39}$	2.68	0.29

adsorption site on a semiconductor surface [1,20,23,24]. As previously mentioned, some of the research suggests a surface exchange reaction between Al and Ga at room temperature. Here, the primary consideration is whether or not atomic aluminum will in fact chemisorb on the Ga-rich GaAs(100) surface and at which sites chemisorption occurs preferentially.

Table 3 lists the nearest surface neighbor adatom bond lengths for all sites considered in this study. Although there is slight variance at some sites, the geometrical predictions are the same for both the 6-311++G** and the HWECP representations of the Al adatom. The Al-Ga bond length of 3.15 Å at the $Ga_{19}As_{15}H_{39}$ + Al cave site is the largest bond length for both representations and the 6-311++G** representation of the $Ga_{19}As_{15}H_{39}$ + Al bridge site has the smallest Al-Ga bond length of 2.27 Å. Table 4 lists the effects on the HOMO-LUMO gaps of the GaAs(100) surface due to adsorption of aluminum. Given the relevance of these gaps in the type of calculations performed here, we however believe that a reasonable *qualitative* picture can be obtained by observing the trends found in these gaps. With the exception of the $Ga_4As_4H_{12}$ + Al sites, all the HOMO-LUMO gaps increase in value, from 0.14 eV for Al adsorption on the $Ga_{19}As_{15}H_{39}$ cluster at the cave site to 4.00 eV for Al adsorption on the $Ga_7As_6H_{19}$ cluster at the bridge site for the 6-311++G** representation of the Al adatom. The same trend is observed with the HWECP representation of the Al adatom, with the lowest value of 0.24 eV for Al adsorption on the $Ga_{19}As_{15}H_{39}$ cluster at the cave site to the highest value of 4.36 eV for Al adsorption on the $Ga_7As_6H_{19}$ cluster at the bridge site. Our results thus suggest, in general, *a possible transition to insulating behavior for the GaAs(100) surface due to aluminum adsorption.*

As observed by Bachrach [10] and by Chadi [11], the GaAs(100)-(2×1) surface is non-metallic upon deposition of a fraction of a monolayer of Al. There appears to be no correlation between chemisorption energy and HOMO-LUMO gap for Al adsorption on the GaAs(100) surface.

We have also carried out an analysis of the atomic charge distributions using Mulliken population analysis [38]. While the magnitudes of the charge exchange between the two representations of the Al adatom vary, the general trends between the two treatments are the same. The 6-311++G** treatment of the Al atom predicts that the sites with the largest transfer of charge from the Al adatom are the $Ga_{19}As_{15}H_{39}$ + Al 5a and 5b trough sites with $0.81e$ and $0.82e$ of charge transfer respectively. These sites are then followed by the $Ga_5As_6H_{16} + Al$ trough site with a charge transfer of $0.53e$ from the Al adatom. Similarly, for the HWECP treatment of the Al adatom, the $Ga_{19}As_{15}H_{39}$ + Al 5a and 5b trough sites yield the greatest charge transfer from the Al adatom with $0.63e$ and $0.61e$ charge transfer respectively, followed by the $Ga_5As_6H_{16}$ + Al trough site with $0.43e$ of charge transfer from the Al adatom. In general, for all considered clusters, the surface Ga atoms tend to gain charge near the site of chemisorption and second layer As atoms tend to gain charge as well. The charge transfer to the third layer is negligible. The negligible charge transfer to the third layer Ga-atoms of the remaining chemisorbed clusters suggests that the three layer cluster models used in this study are sufficient to study the surface adsorption properties of the GaAs(100) surface and possibly other III-V compound semiconductor surfaces.

3 Conclusions

In summary, we have carried out ab initio cluster calculations to study aluminum chemisorption on the Ga-rich GaAs(100) surface. Comparison with the experimental binding energy value of 2.06 ± 0.05 eV for bulk GaAs [39] suggests that the $Ga_7As_6H_{19}$ cluster with E_b(UMP2) = 2.00 eV is the optimal cluster for the (2×1) surfaces considered in this study followed by the $Ga_7As_6H_{16}$ cluster with E_b(UMP2) = 1.95 eV, $Ga_4As_4H_{12}$ with E_b(UMP2) = 1.94 eV, and the $Ga_5As_6H_{16}$ cluster with E_b(UMP2) = 1.85 eV. As the $Ga_{19}As_{15}H_{39}$ cluster was the only representation of the $\beta(4 \times 2)$ surface considered, it is the optimal cluster for the representation of the $\beta(4 \times 2)$ surface in this study with E_b(UMP2) = 1.90 eV. The binding energies, as expected, oscillate with the number of atoms. It was observed that for the five high symmetry sites considered, all sites are possible candidates for chemisorption. For the (2×1) and $\beta(4 \times 2)$ surfaces considered in this study, the trough site appears to be the most favored site for chemisorption with $E_{c(UMP2)}(Ga_5As_6H_{16} + Al) = 4.10$ eV and $E_{c(UMP2)}(Ga_{19}As_{15}H_{39} + Al) = 4.84$ eV at the all-electron level of theory for the Al adatom. Same conclusions prevail at the pseudopotential basis set level, with chemisorption energies of 3.97 eV and 4.73 eV, respectively. The distance of the adatom from the nearest surface neighbor was found to lie between 2.27 to 3.15 Å and the HOMO-LUMO gap was found to vary between 2.53 to 6.06 eV at the all-electron basis set level for the Al adatom. At the pseudopotential level, the distance of the adatom from the nearest surface neighbor was found to lie between 2.43 to 3.15 Å and the HOMO-LUMO gap was found to vary between 2.63 to 6.42 eV. As a result of adsorption, with the exception of the smallest $Ga_4As_4H_{12}$ clusters, the gap increased for all sites considered suggesting a possible transition to insulating behavior of the Ga-rich GaAs(100) surface. Mulliken population analysis indicates that in all cases the Al adatom loses charge. This charge loss is generally gained mostly by surface Ga atoms followed by the second layer As atoms. Further investigations including surface and subsurface relaxation coupled with possibly an increase in the number of layers is warranted to gain a more complete understanding of the complex interactions of Al with the GaAs(100) surface. Obviously, the computational costs will rise dramatically for such studies, specifically for large clusters. Preliminary studies for the (2×1) surface with complete reconstruction and relaxation indicates that the optimal position of the Al adatom is 2.7 Å as compared to 2.5 Å in this study and the chemisorption energy is 1.39 eV to be compared with 1.20 eV obtained here. It is expected that similar shifts will occur for all positions and *at least*, the qualitative trends in this work will be valid in future studies.

The authors gratefully acknowledge very helpful comments from both referees. This work is partially supported by the Welch Foundation, Houston, Texas (Grant No. Y-1525).

References

1. R. Schailey, *An Ab Initio Cluster Study of Chemisorption of Atomic Cesium and Hydrogen on Reconstructed Surfaces of Gallium Rich Gallium Arsenide (100) Surface,* Ph.D. Dissertation, The University of Texas at Arlington (1999); R. Schailey, A.K. Ray, J. Chem. Phys. **111**, 8628 (1999); R. Schailey, A.K. Ray, Comp. Mat. Sci. **22**, 169 (2001)
2. M.L. Mayo, *A Many Body Perturbation Theoretic Study of Atomic Oxygen and Aluminum Chemisorption on GaAs (100) (2×1) and β (4×2) Surfaces,* M.S. Thesis, The University of Texas at Arlington (2003); M.L. Mayo, A.K. Ray, submitted for publication
3. E.J. Mele, J.D. Joannopoulos, Phys. Rev. Lett. **42**, 1094 (1979); E.J. Mele, J.D. Joannopoulos, J. Vac. Sci. Tech. **16**, 1154 (1979)
4. S.J. Eglash, M.D. Williams, P.H. Mahowald, N. Newman, I. Lindau, W.E. Spicer, J. Vac. Sci. Tech. B **2**, 481 (1984)
5. J.P.A. Charlesworth, R.W. Godby, R.J. Needs, Phys. Rev. Lett. **70**, 1685 (1993)
6. S.A. Lourenço, I.F.L. Dias, J.L. Duarte, E. Laureto, F.A. Meneses, J.R. Leite, I. Mazzaro, J. Appl. Phys. **89**, 6159 (2001)
7. C. Berthod, N. Binggeli, A. Baldereschi, Phys. Rev. B **68**, 085323 (2003)

8. R. Ludeke, G. Landgren, J. Vac. Sci. Tech. **19**, 667 (1981)
9. W.-C. Chen, N.G. Fazleev, A.H. Weiss, Rad. Phys. Chem. **68**, 619 (2003)
10. R.Z. Bachrach, R.S. Bauer, P. Chiaradia, G.V. Hansson, J. Vac. Sci. Tech. **19**, 335 (1981)
11. D.J. Chadi, J. Vac. Sci. Tech. A **5**, 834 (1987)
12. D.K. Biegelsen, R.D. Bringans, J.E. Northrup, L.-E. Swartz, Phys. Rev. B **41**, 5701 (1990)
13. J.E. Northup, S. Froyen, Phys. Rev. Lett. **71**, 2276 (1993)
14. W.G. Schmidt, F. Bechstedt, J. Bernholc, Appl. Surf. Sci. **190**, 264 (2002)
15. J.J. Kolodziej, B. Such, M. Szymonski, F. Krok, Phys. Rev. Lett. **90**, 226101 (2003)
16. C. Sgiarovello, N. Binggeli, A. Baldereschi, Phys. Rev. B **69**, 035320 (2004)
17. S.-H. Lee, W. Moritz, M. Scheffler, Phys. Rev. Lett. **85**, 3890 (2000)
18. C. Kumpf, L.D. Marks, D. Ellis, D. Smilgies, E. Landemark, M. Nielsen, R. Feidenhans'1, J. Zegenhagen, O. Bunk, J.H. Zeysing, Y. Su, R.L. Johnson, Phys. Rev. Lett. **86**, 3586 (2001); C. Kumpf, D. Smilgies, E. Landemark, M. Nielsen, R. Friedmans'1, O. Bunk, J.H. Zeysing, Y. Su, R.L. Johnson, L. Cao, J. Zegenhagen, B.O. Fimland, L.D. Marks, D. Ellis, Phys. Rev. B **64**, 075307 (2001)
19. K. Seino, W.G. Schmidt, F. Bechstedt, J. Bernholc, Surf. Sci. **507-510**, 406 (2002)
20. S. Kunsági-Máte, C. Schür, T. Marek, H.P. Strunk, Phys. Rev. B **69**, 193301 (2004)
21. G. Pacchioni, P.S. Bagus, F. Parmigiani, Editors, *Cluster Models for Surface and Bulk Phenomena* (Plenum, New York, 1992)
22. *Physics and Chemistry of Finite Systems: from Clusters to Crystals*, edited by P. Jena, S.N. Khanna, B.K. Rao (Kluwer Publishing, The Netherlands, 1991), *Science and Technology of Atomically Engineered Materials*, edited by P. Jena et al. (World Scientific, Singapore, 1996)
23. K.M. Song, *An Ab Initio Study of Alkali Metal Adsorption on Gallium Arsenide (110) Surface,* Ph.D. Dissertation, The University of Texas at Arlington (1994); K.M. Song, D.C. Khan, A.K. Ray, Phys. Rev. B **49**, 1818 (1994); K.M. Song, A.K. Ray, Phys. Rev. B **50**, 14255 (1994); K.M. Song, A.K. Ray, J. Phys: Condens. Matter **6**, 9571 (1994); K.M. Song, A.K. Ray, J. Phys: Condens. Matter **8**, 6617 (1996)
24. M. Panda, *Interactions of Alkali Atom with the GaAs (110) Surface: A Density Functional Approach,* M.S. Thesis, The University of Texas at Arlington (1997); M. Panda, A.K. Ray, J. Vac. Sci. Tech. A **17**, 2647 (1999)
25. J. Goldstone, Proc. R. Soc. Lond. A **239**, 267 (1956)
26. P.O. Löwdin, J. Math. Phys. **6**, 1341 (1965); P.O. Löwdin, Phys. Rev. **139**, A357 (1965)
27. R.J. Bartlett, Ann. Rev. Phys. Chem. **32**, 359 (1981)
28. W.J. Hehre, L. Random, P.v.R. Schleyer, J.A. Pople, *Ab Initio Molecular Orbital Theory* (Wiley, New York, 1982)
29. A. Szabo, N.S. Ostlund, *Modern Quantum Chemistry* (MacMillian, New York, 1982)
30. E.R. Davidson, D. Feller, Chem. Rev. **86**, 681 (1986)
31. P.J. Hay, W.R. Wadt, J. Chem. Phys. **82**, 284 (1985)
32. *CRC Handbook of Chemistry and Physics*, edited by D.R. Lide, 83rd edn. (CRC Press, Cleveland, 2002)
33. S. Dimon, M. Duran, J.J. Danenberg, J. Chem. Phys. **105**, 11024 (1996); S.F. Boys, M. Bernardi, Mol. Phys. **19**, 553 (1970)
34. M.J. Frisch et al., *Gaussian 98* (Revision A.9), Gaussian Inc., Pittsburgh PA, 1998
35. S. Nonoyama, Y. Aoyagi, S. Namba, Jap. J. Appl. Phys. **31**, 1298 (1992)
36. J. Guo-Ping, H.E. Ruda, J. Appl. Phys. **79**, 3758 (1996)
37. R.C. Binning Jr, L.A. Curtiss, J. Comp. Chem. **11**, 1206 (1990); M.P. McGrath, L. Radom, J. Chem. Phys. **94**, 511 (1991); L.A. Curtiss, M.P. McGrath, J.-P. Blaudeau, N.E. Davis, R.C. Binning Jr, L. Radom, J. Chem. Phys. **103**, 6104 (1995)
38. R.S. Mulliken, J. Chem. Phys. **23**, 1833 (1955); R.S. Mulliken, J. Chem. Phys. **23**, 1841(1955); R.S. Mulliken, J. Chem. Phys. **23**, 2338 (1955); R.S. Mulliken, J. Chem. Phys. **23**, 2343 (1955)
39. G.W. Lemire, G.A. Bishea, S.A. Heidecke, M.D. Morse, J. Chem. Phys. **92**, 121 (1990)